Quantum Chemical Analysis of the Thermodynamics of 2D Cluster Formation of *n*-Carboxylic Acids at the Air/Water Interface

Yu. B. Vysotsky,[†] D. V. Muratov,[†] F. L. Boldyreva,[‡] V. B. Fainerman,[§] D. Vollhardt,*[,||] and R. Miller[||]

Donetsk National Technical University, 58 Artema Str., 83000 Donetsk, Ukraine, Donbas Academy of Civil Engineering and Architecture, 2 Derzavina Str., 86123 Makiyivka, Ukraine, Medical Physicochemical Centre, Donetsk Medical University, 83003 Donetsk, Ukraine, and Max Planck Institute of Colloids and Interfaces, D-14424 Potsdam/Golm, Germany

Received: October 11, 2005; In Final Form: January 10, 2006

Within the framework of PM3 molecular orbital approximation the thermodynamic function characteristics for the formation and geometrical structure of monomers, dimers, trimers, and tetramers of nondissociated *n*-carboxylic acids $C_nH_{2n+1}COOH$ with $n = 5-15$ are calculated. It is shown that spontaneous aggregation of homologous fatty acids for the homologues with carbon atoms numbers $n \geq 13$ at the air/water interface can take place, leading to the formation of infinite plane rectangular clusters, whereas for the homologues with $n < 11$ spontaneous decomposition of large aggregates is energetically preferable. At the same time, the formation of trimers is more probable for the lower homologues ($8 < n < 13$). These results agree well both with the experimental data reported by various authors and with thermodynamic models developed earlier for soluble and insoluble monolayers. The slopes of the regressions calculated for the dependencies of the thermodynamic parameters on the alkyl chain length for all the clusters considered are all equal to each other. This fact indicates that the contributions of the CH_2 groups to the thermodynamic characteristics of alcohols and acids are the same, and the differences in the formation of clusters by these substances should be attributed only to the differences in the structure and interactions of relevant functional groups. Therefore, it enables one to describe both acids and alcohols within the framework of the developed method, and it makes it possible to extend the proposed approach onto other classes of amphiphilic compounds.

Introduction

The homologous series of *n*-alcohols and *n*-carboxylic acids can serve as good models for the study of general features characteristic for the behavior of surfactants at interfaces. The results obtained for soluble fatty acids ($C_nH_{2n+1}COOH$) in various studies[1−4] were discussed in ref 5 in the framework of Frumkin's and aggregation theoretical models. It was shown that, for carboxylic acids of lower chain lengths (C_7-C_9), two theoretical models provide an equally good description of the experimental data. For decanoic and dodecanoic acids, the aggregation model leads to an essentially smaller deviation from the experimental data (by a factor of 2 for dodecanoic acid) than the Frumkin model, and it yields aggregation numbers of $m = 3, 4$. Therefore, a certain similarity exists in the behavior of fatty acids and alcohols. For shorter alkyl chains the system is better described by the Frumkin model, whereas for longer alkyl chains the behavior becomes more "aggregation-like" . However, condensation sets in for the acids only at C_{13},[6,7] whereas for *n*-alcohols this is observed at alkyl chains $\geq C_{12}$.

In the present study we propose a new theoretical adsorption model which assumes aggregation in the adsorbed monolayer and nonideality of entropy of the mixed monolayer. It is shown by processing the experimental surface tension isotherms for *n*-alkanoic acids C_5-C_{11} reported in ref 8 that for C_7-C_{11} fatty acids the formation of trimers is most probable.

On the other hand, using quantum chemical methods it is possible to calculate directly enthalpy ΔH_m^{cl}, entropy ΔS_m^{cl} and Gibbs energy ΔG_m^{cl}, of the dimerization and clusterization in finite and infinite clusters. In our previous studies,[9−12] for example, using fatty alcohols, we compared the results obtained for the thermodynamic parameters of clusterization from quantum chemical calculations with the experimental data. It was shown that both the kinetic and thermodynamic behavior of the molecules during the cluster formation and recrystallization are governed by the entropy factor.[11−14] It was noted that for fatty alcohols the increase of the stability of clusters with the increase of the chain length is due to the H−H interactions between alkyl chains, which could be quite satisfactory described in the PM3 parametrization. A similar situation was also observed for polyfluorinated alcohols with the general formula $C_nF_{2n+1}CH_2CH_2OH$.[15] In this case the polyfluorinated alcohols exhibit a characteristic helical structure, and the increase of the stability of the clusters with the increase of the *n* value is caused by F−F interactions.

In the present work we studied the thermodynamic characteristics of the cluster formation for fatty acids with the general formula $C_nH_{2n+1}COOH$, $n = 5-15$.

Methods

It was demonstrated on the basis of fatty and fluorinated alcohols,[9−15] that among the methods in the series MNDO/3,

* Corresponding author.
[†] Donetsk National Technical University.
[‡] Donbas Academy of Civil Engineering and Architecture.
[§] Donetsk Medical University.
[||] Max Planck Institute of Colloids and Interfaces.

10.1021/jp055804l CCC: $33.50
Published on Web 02/14/2006

MNDO, AM1, and PM3, the PM3 method yields the lowest error with respect to the description of van der Waals complexes. Therefore, in this work the theoretical studies of the cluster formation of fatty acids were performed using the PM3 molecular orbital approximation, implemented in the Mopac2000 (Fujitsu Limited) software[16] run on an IBM PC. The search for minima at the potential energy surface was performed using the modified Broyden−Fletcher−Goldfarb−Shanno (BFGS) procedure. The minima points were identified as those for which the negative eigenvalues in the Hessian matrix are absent. The restricted Hartree−Fock method was applied to the calculation of wave function. For the van der Waals molecules the low frequency (several tens of reciprocal centimeters) intermolecular vibrations are characteristic.[17,18] As previously shown[9−15] these vibrations are essential for an adequate description of the cluster formation entropy. Therefore, the restrictions relative to the calculation of the vibration contributions to the entropy, which are implemented in the most recent versions of the MOPAC software and imply the neglect of the contributions from vibrations with frequencies below 100 cm^{-1}, are incorrect in the present case, and in our calculations of entropy values, these terms were accounted for directly. The analysis of dipole−dipole interactions between the functional groups was performed using interactive functions implemented in the HyperChem Professional 7 and WinMopac software. For the statistical processing of the experimental results of the computation, the MS Excel program environment was used.

Results and Discussion

Monomers. In contrast to fatty alcohols, the thermodynamic characteristics of the monomers of fatty acids are essentially dependent on the geometric configuration of the carboxyl group. Therefore, the conformation analysis of the relevant monomers was performed at the first stage of our study of the thermodynamic characteristics of cluster formation.

The potential energy surface of the palmitic acid molecule is illustrated in Figure 1. Here the energy in kJ/mol is plotted along the *Z* axis vs the values of torsion angles which are shown in Figure 2. The torsion angles were varied with the increment of 15° in the ranges: ∠OCCC along the *X* axis within the range 180−540°, ∠HOCC along the *Y* axis within the range 120−435°. The initial point for the surface construction was the molecular geometry with the values of torsion angles resulting from the optimization: ∠OCCC = −0.85098°, and ∠HOCC = −0.02971°. The construction of the potential surface was performed without optimization.

It is seen from Figure 1 that two minima exist on the surface: the global minimum at ∠OCCC = 0°, ∠HOCC = 180° and the local minimum at ∠OCCC = 0°, ∠HOCC = 0°. The optimization in the neighborhood of a point of the global minimum results in the monomer 1 structure (see Figure 3), which is stabilized by the intramolecular hydrogen bond formed between the carbonyl oxygen atom and the hydroxyl hydrogen atom involved in the carbonyl group. The optimization in the local minimum domain showed that three other stable conformations can exist, the monomers 2, 3, and 4, with the structure stabilized due to the intramolecular H−H bonds which are formed between the hydroxyl hydrogen atom and the α,β-hydrogen atoms of the alkyl chain. The molecular geometries of these stable conformers are shown in Figure 3.

In Table 1m the values of the standard thermodynamic characteristics ΔH^0_{298}, ΔS^0_{298}, and ΔG^0_{298} for the formation of monomers of *n*-fatty acids $C_nH_{2n+1}COOH$ (n = 5−15) from the elementary substances, calculated with the PM3 semiempiric

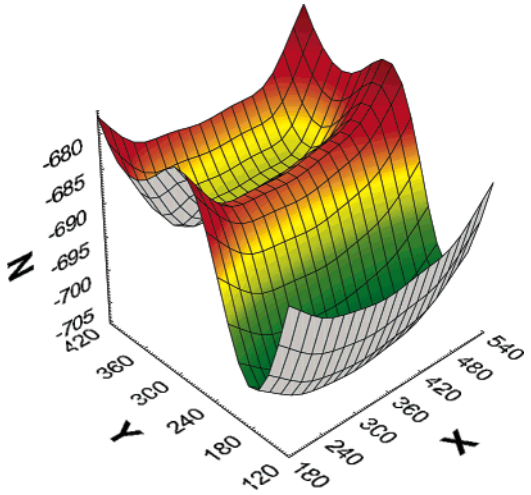

Figure 1. Potential energy surface for the palmitic acid monomer.

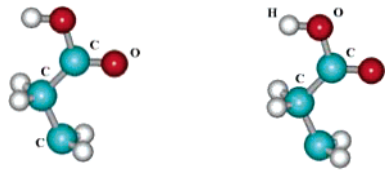

Figure 2. Torsion angles in the carboxyl group: (a) ∠OCCC; (b) ∠HOCC.

method, are compared with the experimental values reported in refs 19−21. It follows from Table 1 that the root-mean-square error relative to the description of experimental data for ΔH^0_{298} is 5.9−10.3 kJ/mol, which is lower than the corresponding error (23 kJ/mol) for *n*-alcohols.[9−12] The calculation of the standard entropies of the formation ΔS^0_{298} yields a somewhat larger error. This can be ascribed to the fact that the free rotation of alkyl groups was neglected.[9] The account for the entropy contribution from the free rotation of alkyl groups leads to a better agreement with the experimental data. The root-mean-square error for the experimental value of ΔS^0_{298} decreases to 3−13 J/mol·K which yields a correction of 6.1 J/mol·K per one CH_2 group. This value is almost equal to that of 6.6 J/mol·K proposed for alcohols.[9] Therefore, for unification purposes, we use this last value. In Table 1, the corrected values of entropies and Gibbs energies are shown in parentheses. In this case the root-mean-square error for the description of experimental values of Gibbs' standard energy of formation is 5.1−13.2 kJ/mol for the various conformers of fatty acids.

Similar to the alcohols, for all conformers of fatty acids the ΔH^0_{298}, ΔS^0_{298}, and ΔG^0_{298} values exhibit a linear dependence on the alkyl chain length. Corresponding regression coefficients and standard root-mean-square errors are listed in Table 2, and compared to the values obtained for alcohols in refs 9−12. All regression coefficients exceed 0.9999. The fact that the correlation is so high enables one to distinguish between the contributions of the alkyl chain methylene fragments and the remainder of the molecule to the thermodynamic parameters. Similar correlations exist also for the experimental values, see Table 2. It should be noted that, for each corresponding thermodynamic characteristic of all the regressions considered (and also for alcohols), the slopes for the corresponding thermodynamic characteristics are very close to each other. This could be regarded as evidence for the fact that the contributions of CH_2 groups to the thermodynamic properties for all conformers studied are equal both in alcohols and acids.

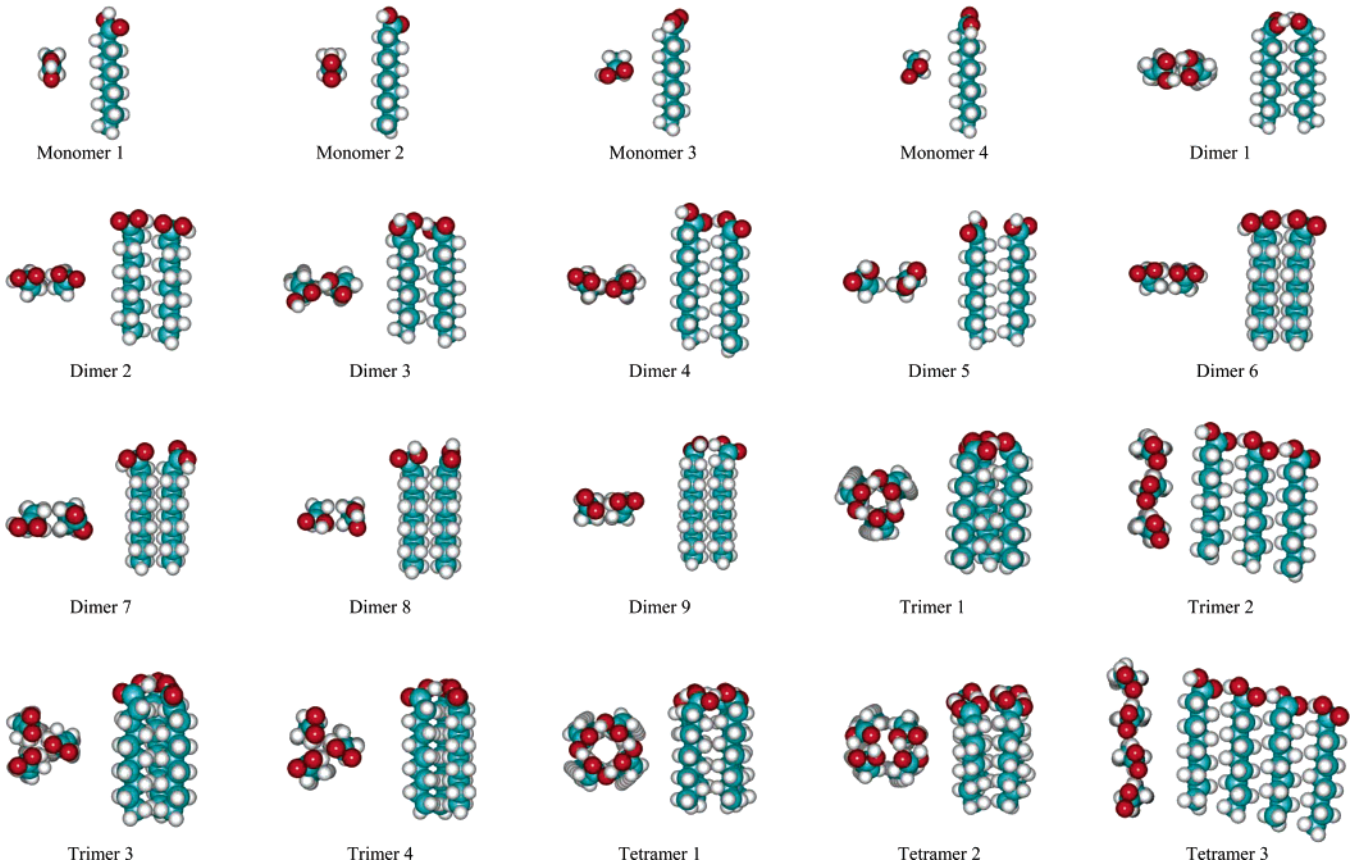

Figure 3. Different structures of carboxylic acid monomers and clusters (schematically).

Dimers, Trimers, and Tetramers. The dimers and trimers of different structures shown in Figure 3 were obtained from monomers 1− 4 by rotating of one monomer around the axis of the second monomer or dimer. The structures shown in Figure 3 correspond to the potential surface minima. In these minima, an additional optimization of the geometric structure of the studied clusters was performed. The optimum geometry of the alkyl chain was found to be the same as that obtained earlier for alcohols.[9−12] This can be attributed to the fact that the stability of molecular clusters of acids is determined by the same types of H−H interactions as in clusters composed of alcohol molecules. The ternary and quaternary H−H interactions lead to less stable clusters.[9,10] Therefore, in the present work, we consider mainly the cluster structures which correspond to binary interactions between hydrogen atoms.

The presence of an additional functional center (oxygen ketone atom) in carbon acids leads to an essential extension of the conformational space. Therefore, an additional analysis has been be performed to determine the geometry of the carboxyl groups and their relative positions in the molecular cluster which are energetically most preferable. The geometry of carboxyl groups in the monomers was initially defined as the optimal structure for conformers 1 and 2 which correspond to the presence and absence of intramolecular hydrogen bonds, respectively. The geometrical characteristics subjected to the optimization are the relative position of carboxyl groups and the relative position of the alkyl chains. The potential energy surface for one of the most energetically preferable dimers (dimer 2) is presented in Figure 4. The initial geometry for the construction of the potential surface was the optimized structure of dimer 2 without intramolecular hydrogen bonds, for which the torsion angles ∠OCCC for the first and second monomers were −111.98 and −75.22°, respectively. It is seen from Figure 4 that one minimum exists at the surface, which corresponds to the formation of the intermolecular hydrogen bond according to the "head-alkyl chain" mechanism with the coordinates 240°, 285°. The total optimization of the dimer was made in this minimum point. Its geometrical structure is shown in Figure 3 (dimer 2). A similar procedure was performed for all clusters studied.

Enthalpy $\Delta H_m^{cl} = \Delta H_m - m\Delta H_1$ and entropy $\Delta S_m^{cl} = \Delta S_m - m\Delta S_1$ of the cluster formation and Gibbs' energy of cluster formation $\Delta G_m^{cl} = \Delta H_m^{cl} - T\Delta S_m^{cl}$ for dimers, trimers, and tetramers of fatty acids with normal structure are listed in Table 3. Here and below, m denotes the number of monomers in a cluster. Figure 3 illustrates the geometry of the calculated structures for $n = 9$. In this case, the initial structures chosen for the construction of clusters are monomer 1, which possesses the intramolecular hydrogen bond, and monomer 2, which does not possess this bond. monomers 3 and 4 have the energetic and structural characteristics quite similar to those of monomer 2, and therefore we did not consider the cluster formation involving these monomers. In each case, for calculating ΔH_m^{cl}, ΔS_m^{cl}, the thermodynamic characteristics of those particular monomers of which the cluster is formed, are subtracted from the resulting value. For example, for dimer 1 and trimer 1, the data for monomer 2 are used, for dimer 5 and dimer 8 the data for monomer 2 are subtracted, and so on.

Similarly to what was shown earlier for alcohols,[9−12] in the present case for each cluster either linear or stepwise dependence of ΔH_m^{cl}, ΔS_m^{cl}, and ΔG_m^{cl} values on number and type of H−H interactions in the molecule is observed. The shape of the dependence is governed by the type of interactions in the hydrocarbon chains. The correlation coefficients of the regressions for ΔH_m^{cl} exceed 0.994, and for ΔS_m^{cl} these coefficients are above 0.98, with standard deviations within the ranges of

TABLE 1: Standard Thermodynamic Characteristics for the Formation of Carboxylic Acid Monomers

	standard enthalpy of formation ΔH^0_{298}, kJ/mol				
molecule	conformation 1	conformation 2	conformation 3	conformation 4	experimental data[7−9]
$C_5H_{13}COOH$	−512.88	−501.95	−504.22	−504.77	−511.9
$C_6H_{15}COOH$	−535.52	−524.56	−526.86	−527.42	−536.2
$C_7H_{17}COOH$	−558.20	−547.25	−549.52	−550.07	−556.0
$C_8H_{19}COOH$	−580.86	−569.91	−572.18	−572.73	−577.3
$C_9H_{21}COOH$	−603.54	−592.59	−594.85	−595.40	−594.3
$C_{10}H_{23}COOH$	−626.22	−615.26	−617.53	−618.07	−614.6
$C_{11}H_{25}COOH$	−648.90	−637.94	−640.20	−640.75	−640.0
$C_{12}H_{27}COOH$	−671.58	−660.62	−662.88	−663.43	−660.2
$C_{13}H_{29}COOH$	−694.26	−683.31	−685.56	−686.10	−683.0
$C_{14}H_{31}COOH$	−716.94	−705.98	−708.24	−708.79	−699.0
$C_{15}H_{33}COOH$	−739.63	−728.66	−730.92	−731.47	−723.0
	standard entropy of formation ΔS^0_{298}, J/mol·K				
molecule	conformation 1	conformation 2	conformation 3	conformation 4	experimental data[7−9]
$C_5H_{13}COOH$	426.30 (459.31)	420.98 (453.98)	416.05 (449.05)	409.94 (442.94)	441.0
$C_6H_{15}COOH$	458.07 (497.67)	453.06 (492.66)	448.67 (488.27)	442.47 (482.07)	480.0
$C_7H_{17}COOH$	489.10 (535.30)	485.01 (531.21)	480.56 (526.77)	474.42 (520.62)	520.0
$C_8H_{19}COOH$	520.56 (573.36)	516.80 (569.60)	512.53 (565.33)	506.81 (559.61)	559.0
$C_9H_{21}COOH$	552.80 (612.20)	549.14 (608.54)	544.61 (604.01)	538.52 (597.92)	599.0
$C_{10}H_{23}COOH$	585.25 (651.25)	580.86 (646.86)	576.66 (642.66)	570.41 (636.41)	638.0
$C_{11}H_{25}COOH$	616.28 (688.88)	612.72 (685.32)	608.25 (680.85)	602.29 (674.89)	677.4
$C_{12}H_{27}COOH$	648.55 (727.75)	644.37 (723.57)	640.39 (719.59)	634.06 (713.26)	717.0
$C_{13}H_{29}COOH$	679.60 (765.40)	676.05 (761.85)	671.31 (757.11)	665.70 (751.50)	754.0
$C_{14}H_{31}COOH$	710.15 (802.55)	707.52 (799.92)	703.68 (796.08)	696.77 (789.17)	796.0
$C_{15}H_{33}COOH$	742.22 (841.22)	738.91 (837.91)	734.79 (833.79)	728.04 (827.04)	833.0
	standard Gibbs' energy of formation ΔG^0_{298}, kJ/mol				
molecule	conformation 1	conformation 2	conformation 3	conformation 4	experimental data[7−9]
$C_5H_{13}COOH$	−335.05(−344.88)	−322.52 (−332.36)	−323.32 (−333.16)	−322.06 (−331.89)	−338.4
$C_6H_{15}COOH$	−326.52 (−338.32)	−314.07 (−325.87)	−315.06 (−326.86)	−313.77 (−325.57)	−333.7
$C_7H_{17}COOH$	−317.81 (−331.58)	−305.65 (−319.41)	−306.59 (−320.36)	−305.31 (−319.08)	−324.8
$C_8H_{19}COOH$	−309.23 (−324.96)	−297.15 (−312.89)	−298.15 (−313.89)	−297.00 (−312.74)	−317.1
$C_9H_{21}COOH$	−300.88 (−318.58)	−288.84 (−306.54)	−289.75 (−307.45)	−288.49 (−306.19)	−305.4
$C_{10}H_{23}COOH$	−292.60 (−312.27)	−280.33 (−300.00)	−281.35 (−301.02)	−280.03 (−299.70)	−296.7
$C_{11}H_{25}COOH$	−283.90 (−305.54)	−271.88 (−293.52)	−272.80 (−294.44)	−271.58 (−293.21)	−293.2
$C_{12}H_{27}COOH$	−275.57 (−299.17)	−263.36 (−286.96)	−264.44 (−288.04)	−263.10 (−286.70)	−284.6
$C_{13}H_{29}COOH$	−266.87 (−292.44)	−254.86 (−280.43)	−255.70 (−281.26)	−254.57 (−280.14)	−277.8
$C_{14}H_{31}COOH$	−258.03 (−285.57)	−246.28 (−273.82)	−247.39 (−274.93)	−245.89 (−273.42)	−265.7
$C_{15}H_{33}COOH$	−249.64 (−279.14)	−237.69 (−267.19)	−238.72 (−268.22)	−237.26 (−266.76)	−260.1

0.02−4.05 kJ/mol and 1.0−12.9 J/mol·K, respectively. For example, the regression dependencies for dimer 2 are

$$\Delta H_m^{\text{dim}} = -(12.60 \pm 0.33) - (5.14 \pm 0.03)(2\{n/2\}) \text{ kJ/mol}; \quad (R = 0.9998;\ S = 0.32 \text{ kJ/mol})$$

$$\Delta S_m^{\text{dim}} = -(129.11 \pm 2.16) - (11.26 \pm 0.19)(2\{n/2\}) \text{ J/(mol·K)}; \quad (R = 0.9986;\ S = 2.08 \text{ J/(mol·K)}) \quad (1)$$

where the symbol {...} denotes the integer part of a number and n is the number of carbon atoms in the hydrocarbon chain {residuum}.

It is seen from Table 3 that for dimer 1 negative ΔG_m^{cl} values correspond to the hydrocarbon chain length which is lowest among all dimers. Therefore, for this cluster the spontaneous formation of a dimer from monomers should take place at the lowest n value: $n = 12$. This can be explained by the fact that this dimer involves a maximum number (two, cf. Figure 3) of intermolecular hydrogen bonds. The clusters shown in Figure 3 and Table 3 are ordered according to the increase of the number of monomers in a cluster (m). Within one m value they are ordered according to the increase of the minimum n value for which a spontaneous formation of clusters from monomers should take place.

In the dimer series, the second one is dimer 2, which possesses only one intermolecular hydrogen bond and has no intramolecular hydrogen bonds. Note that in this cluster the H−H bonds of the 1a type (see ref 10) are formed between the methylene groups which occupy the same positions in the hydrocarbon chains of adjacent molecules. Also the formation of dimer 4 clusters is possible, where the bonds are formed between the methylene groups of the monomers which are "shifted" vertically relative to one another by one group. This bonding type leads to the situation in which dimer 4 is inclined by 80° with respect to the interface, unlike dimer 2, which is oriented perpendicularly to the interface. Structures with a similar organization were observed earlier in fatty alcohol clusters.[22] Whereas dimer 4 stands farther in the dimer series than dimer 2 (i.e., its spontaneous formation should take place at a larger n value), the trimers and tetramers formed of dimer 4 (see trimer 2 and tetramer 4) stand before the corresponding dimer 2-type clusters in the trimer and tetramer series. This should be attributed to the fact that the attachment of the third monomer to dimer 2 results in the decrease of the H−H contacts number per one molecule in the cluster, and also in the formation of additional intermolecular repulsion between oxygen atoms of carboxyl groups, see Figure 3.

One and two intramolecular hydrogen bonds, respectively, are formed in dimer 3 and dimer 5. In dimers 6−9, the interaction between the hydrogen atoms in hydrocarbon chains takes place according to the 1b type,[10] and ΔG_m^{cl} energies calculated for these dimers are essentially higher than those for other dimers. Similar to the alcohols, for these dimers 6−9 a linear dependence of ΔH_m^{cl}, ΔS_m^{cl}, and ΔG_m^{cl} on the number

TABLE 2: Correlation Equations in the Form: $(y \pm S) = (a \pm \Delta a)n + (b \pm \Delta b)$ for Monomers of Fatty Acids and Alcohols[9−12]

conformer	thermodynamic parameter	$(a \pm \Delta a)$	$(b \pm \Delta b)$	S
fatty acid monomer 1	ΔH^0_{298}, kJ/mol	−22.68 ± 0.00	−399.47 ± 0.01	0.01
	ΔS^0_{298}, J/(mol·K)	38.23 ± 0.05	268.19 ± 0.57	0.57
	ΔG^0_{298}, kJ/mol	6.56 ± 0.02	−377.66 ± 0.17	0.17
fatty acid monomer 2	ΔH^0_{298}, kJ/mol	−22.67 ± 0.00	−388.53 ± 0.02	0.02
	ΔS^0_{298}, J/(mol·K)	38.41 ± 0.04	262.37 ± 0.38	0.38
	ΔG^0_{298}, kJ/mol	6.51 ± 0.01	−364.99 ± 0.10	0.10
fatty acid monomer 3	ΔH^0_{298}, kJ/mol	−22.67 ± 0.00	−390.82 ± 0.02	0.02
	ΔS^0_{298}, J/(mol·K)	38.47 ± 0.04	257.47 ± 0.47	0.47
	ΔG^0_{298}, kJ/mol	6.49 ± 0.01	−365.82 ± 0.13	0.13
fatty acid monomer 4	ΔH^0_{298}, kJ/mol	−22.67 ± 0.00	−391.38 ± 0.02	0.02
	ΔS^0_{298}, J/(mol·K)	38.42 ± 0.06	251.78 ± 0.60	0.60
	ΔG^0_{298}, kJ/mol	6.51 ± 0.02	−364.68 ± 0.16	0.16
alcohols	ΔH^0_{298}, kJ/mol	−22.68 ± 0.00	−214.67 ± 0.00	0.00
	ΔS^0_{298}, J/(mol·K)	38.61 ± 0.05	247.48 ± 0.55	0.55
	ΔG^0_{298}, kJ/mol	6.44 ± 0.02	−178.32 ± 0.16	0.16

of hydrogen atoms in the hydrocarbon radical is observed, rather than a stepwise dependence.

It follows from the calculations made for dimers that the existence of a classical intermolecular hydrogen bond (2a type, see Figure 6) leads to an essential decrease of the ΔH_m^{cl} value, and negative ΔG_m^{cl} values for these clusters correspond to lower n. The higher the number of intermolecular hydrogen bonds of the 2a type per one molecule in a cluster, the lower ΔG_m^{cl} value. Therefore, in the dimer series the first cluster is the cyclic trimer 1, which possesses three intermolecular hydrogen bonds, see Figure 3 and Table 3. Trimerization takes place for this cluster at the lowest value $n = 8$. The next cluster in the trimer series is trimer 2 which possesses two intermolecular hydrogen bonds. This, quite naturally, leads to the fact that for this cluster the ΔG_m^{cl} values become negative at the alkyl chain length $n = 14$. For trimer 3 and trimer 4 the Gibbs' clusterization energy is significantly higher than for trimer 1 and trimer 2, because in these trimers the 2b type intermolecular oxygen−hydrogen interactions exist which lead to an essential decrease of ΔS_m^{cl}. In trimer 4 for all the methylene fragments of the alkyl chain the triple H−H interaction takes place according to type 1c, see ref 10. This interaction between the hydrocarbon chains of the monomers optimally corresponds to three intermolecular 2b type interactions between the carbonyl groups. Trimer 3 stands before trimer 4 in the trimer series, because ceteris paribus the contributions of 1a type H−H interactions are more energetically advantageous than the 1c type interactions; see ref 10.

Similar to the situation observed for dimers and trimers, in the tetramer series the first ones are the cyclic tetramer 1 and tetramer 2. This can be attributed to the fact that, in this case, a maximum number of hydrogen bonds per one monomer is formed. These correspond to the 2a type oxygen−hydrogen interaction, see Figure 6. Tetramer 1 stands before tetramer 2 in the series because in tetramer 4 a cycle stress does not exist, which is characteristic of structures based on dimer 1 and, in particular, to tetramer 2. Therefore, for tetramer 1 a spontaneous formation of the cluster from monomers takes place at $n = 8$, whereas for tetramer 2 the clusterization occurs only at $n = 13$. Tetramer 3 belongs to the family of clusters based on the dimer 4 structure, and exhibits therefore, all the features characteristic for this family, as explained above.

Large and Infinite Clusters. It follows from Table 3 that, for fatty alcohols, the slopes of the dependencies are in a very good correspondence with the regression coefficients for all the types of interactions between alkyl chains.[9−12] Therefore, similarly to the monomers (cf. Table 2), the increments of methylene fragments and functional groups in the physicochemical parameters could be distinguished from each other, and the

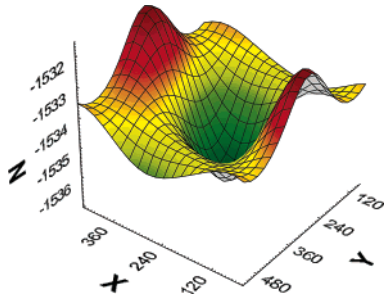

Figure 4. Potential energy surface for the palmitic acid dimer 2.

additive approach developed earlier for fatty alcohols can be extended to the case of fatty acids. Here two approaches are possible: (i) application of the additive scheme used for the description of interactions between the alkyl chains of fatty alcohols,[9−12] incorporating into this scheme of increments which account for the interaction between oxygen and hydrogen atoms of carboxyl groups, or (ii) development of an independent additive scheme which describes the thermodynamic characteristics of the clusterization of fatty acids. These approaches lead to similar values of increments which account for the contribution of methylene fragments to the thermodynamic characteristics of the cluster formation. That means, these approaches provide a similar qualitative description of the dependence of the thermodynamic characteristics on the cluster structure and alkyl chain length. For example, the accuracy in the description of fatty acids in the framework of the second approach is 5.66 kJ/mol ($R = 0.995$) for ΔH_m^{cl} and 19.6 J/(mol·K) ($R = 0.994$) for ΔS_m^{cl}. In this publication the first approach is adopted. It should be noted that this approach enables one to incorporate into this additive scheme the clusters formed by amphiphilic compounds of other classes.

In contrast to the fatty alcohols, the additive scheme for the description of the thermodynamic characteristics of fatty acids should account for also the presence of carbonyl and hydroxyl constituents in the carboxyl group. The presence of carboxyl groups, on one hand, leads to a significant increase in the number of possible types of interactions between CO and OH groups; on the other hand, the different location of COOH groups complicates significantly the selection of relevant interactions in the particular clusters considered. For alcohols, the distance between the hydroxyl groups could be employed as the criterion for the selection, whereas in the present case not only the distances, but also the relative orientation of the functional groups should be taken into account. The selection can be perfprmed on the basis of the analysis of the dipole−dipole contributions to the electrostatic interaction, which arises

TABLE 3: Standard Thermodynamics Characteristics for Cluster Formation of Carboxylic Acid Calculated in the PM3 Approximation

system	ΔH_m^{cl}, kJ/mol	ΔS_m^{cl}, J/(mol·K)	ΔG_m^{cl}, kJ/mol	system	ΔH_m^{cl}, kJ/mol	ΔS_m^{cl}, J/(mol·K)	ΔG_m^{cl}, kJ/mol
			Dimer 1				
$C_5H_{13}COOH$	−44.39	−206.75	17.22	$C_{11}H_{25}COOH$	−74.68	−257.37	2.01
$C_6H_{15}COOH$	−53.76	−224.40	13.11	$C_{12}H_{27}COOH$	−84.37	−271.60	−3.43
$C_7H_{17}COOH$	−54.33	−223.78	12.36	$C_{13}H_{29}COOH$	−84.95	−265.86	−5.72
$C_8H_{19}COOH$	−63.88	−241.25	8.02	$C_{14}H_{31}COOH$	−94.67	−285.50	−9.60
$C_9H_{21}COOH$	−64.45	−241.67	7.56	$C_{15}H_{33}COOH$	−95.26	−282.94	−10.94
$C_{10}H_{23}COOH$	−74.11	−257.61	2.66				
			Dimer 2				
$C_5H_{13}COOH$	−43.19	−194.06	14.64	$C_{11}H_{25}COOH$	−74.04	−266.40	5.35
$C_6H_{15}COOH$	−43.73	−195.47	14.52	$C_{12}H_{27}COOH$	−74.67	−264.82	4.24
$C_7H_{17}COOH$	−53.44	−220.60	12.30	$C_{13}H_{29}COOH$	−84.38	−287.98	1.44
$C_8H_{19}COOH$	−54.00	−219.12	11.30	$C_{14}H_{31}COOH$	−85.02	−284.14	−0.35
$C_9H_{21}COOH$	−63.74	−245.14	9.31	$C_{15}H_{33}COOH$	−94.74	−307.38	−3.14
$C_{10}H_{23}COOH$	−64.33	−242.04	7.80				
			Dimer 3				
$C_5H_{13}COOH$	−38.14	−185.03	17.00	$C_{11}H_{25}COOH$	−69.05	−255.48	7.08
$C_6H_{15}COOH$	−47.86	−209.77	14.65	$C_{12}H_{27}COOH$	−78.80	−279.37	4.45
$C_7H_{17}COOH$	−48.40	−208.87	13.84	$C_{13}H_{29}COOH$	−79.40	−279.95	4.02
$C_8H_{19}COOH$	−58.14	−232.46	11.13	$C_{14}H_{31}COOH$	−89.15	−301.25	0.62
$C_9H_{21}COOH$	−58.67	−231.59	10.35	$C_{15}H_{33}COOH$	−89.75	−297.99	−0.95
$C_{10}H_{23}COOH$	−68.57	−257.85	8.27				
			Dimer 4				
$C_5H_{13}COOH$	−37.44	−173.33	14.21	$C_{11}H_{25}COOH$	−66.62	−246.61	6.87
$C_6H_{15}COOH$	−45.52	−191.98	11.69	$C_{12}H_{27}COOH$	−74.37	−263.66	4.20
$C_7H_{17}COOH$	−46.15	−195.48	12.11	$C_{13}H_{29}COOH$	−77.02	−268.43	2.97
$C_8H_{19}COOH$	−53.85	−213.92	9.90	$C_{14}H_{31}COOH$	−84.73	−288.79	1.33
$C_9H_{21}COOH$	−56.47	−219.92	9.07	$C_{15}H_{33}COOH$	−87.37	−295.57	0.71
$C_{10}H_{23}COOH$	−64.04	−240.52	7.63				
			Dimer 5				
$C_5H_{13}COOH$	−28.87	−149.40	15.65	$C_{11}H_{25}COOH$	−59.75	−238.42	11.30
$C_6H_{15}COOH$	−29.46	−155.81	16.97	$C_{12}H_{27}COOH$	−60.32	−241.91	11.76
$C_7H_{17}COOH$	−39.13	−180.66	14.71	$C_{13}H_{29}COOH$	−70.06	−265.43	9.03
$C_8H_{19}COOH$	−39.68	−184.37	15.26	$C_{14}H_{31}COOH$	−70.64	−267.37	9.04
$C_9H_{21}COOH$	−49.43	−211.39	13.56	$C_{15}H_{33}COOH$	−80.38	−292.75	6.86
$C_{10}H_{23}COOH$	−50.00	−216.44	14.50				
			Dimer 6				
$C_5H_{13}COOH$	−45.46	−233.66	24.17	$C_{11}H_{25}COOH$	−82.39	−355.35	23.51
$C_6H_{15}COOH$	−51.66	−254.78	24.26	$C_{12}H_{27}COOH$	−88.54	−375.53	23.37
$C_7H_{17}COOH$	−57.79	−275.34	24.27	$C_{13}H_{29}COOH$	−94.68	−394.23	22.80
$C_8H_{19}COOH$	−63.92	−294.50	23.84	$C_{14}H_{31}COOH$	−100.86	−413.91	22.49
$C_9H_{21}COOH$	−70.07	−315.85	24.05	$C_{15}H_{33}COOH$	−107.02	−432.46	21.85
$C_{10}H_{23}COOH$	−76.22	−335.55	23.77				
			Dimer 7				
$C_5H_{13}COOH$	−30.54	−203.72	30.16	$C_{11}H_{25}COOH$	−66.65	−327.12	30.84
$C_6H_{15}COOH$	−36.49	−224.99	30.56	$C_{12}H_{27}COOH$	−72.86	−345.60	30.13
$C_7H_{17}COOH$	−42.52	−244.45	30.32	$C_{13}H_{29}COOH$	−79.01	−365.37	29.87
$C_8H_{19}COOH$	−48.46	−265.55	30.68	$C_{14}H_{31}COOH$	−85.04	−385.58	29.86
$C_9H_{21}COOH$	−54.50	−286.09	30.75	$C_{15}H_{33}COOH$	−91.21	−404.54	29.35
$C_{10}H_{23}COOH$	−60.36	−306.46	30.96				
			Dimer 8				
$C_5H_{13}COOH$	−30.70	−212.36	32.58	$C_{11}H_{25}COOH$	−67.68	−332.35	31.35
$C_6H_{15}COOH$	−36.89	−233.35	32.65	$C_{12}H_{27}COOH$	−73.83	−354.42	31.79
$C_7H_{17}COOH$	−43.05	−252.14	32.09	$C_{13}H_{29}COOH$	−80.00	−372.58	31.03
$C_8H_{19}COOH$	−49.19	−271.01	31.57	$C_{14}H_{31}COOH$	−86.17	−391.38	30.46
$C_9H_{21}COOH$	−55.37	−291.71	31.56	$C_{15}H_{33}COOH$	−91.77	−410.71	30.62
$C_{10}H_{23}COOH$	−61.51	−312.68	31.67				
			Dimer 9				
$C_5H_{13}COOH$	−26.11	−240.27	45.49	$C_{11}H_{25}COOH$	−62.89	−360.13	44.43
$C_6H_{15}COOH$	−32.25	−260.67	45.43	$C_{12}H_{27}COOH$	−69.04	−378.10	43.64
$C_7H_{17}COOH$	−38.36	−280.37	45.19	$C_{13}H_{29}COOH$	−75.19	−397.25	43.19
$C_8H_{19}COOH$	−44.48	−300.03	44.92	$C_{14}H_{31}COOH$	−81.39	−418.02	43.18
$C_9H_{21}COOH$	−50.61	−320.87	45.01	$C_{15}H_{33}COOH$	−90.94	−446.81	42.21
$C_{10}H_{23}COOH$	−56.78	−340.88	44.80				
			Trimer 1				
$C_5H_{13}COOH$	−108.11	−432.41	20.75	$C_{11}H_{25}COOH$	−193.10	−565.39	−24.61
$C_6H_{15}COOH$	−134.19	−478.95	8.54	$C_{12}H_{27}COOH$	−219.46	−610.67	−37.48
$C_7H_{17}COOH$	−136.29	−478.46	6.29	$C_{13}H_{29}COOH$	−221.55	−611.18	−39.42
$C_8H_{19}COOH$	−162.48	−523.90	−6.36	$C_{14}H_{31}COOH$	−247.85	−661.29	−50.79
$C_9H_{21}COOH$	−164.67	−524.53	−8.36	$C_{15}H_{33}COOH$	−250.03	−655.40	−54.72
$C_{10}H_{23}COOH$	−190.95	−569.94	−21.10				

TABLE 3: Continued

system	ΔH_m^{cl}, kJ/mol	ΔS_m^{cl}, J/(mol·K)	ΔG_m^{cl}, kJ/mol	system	ΔH_m^{cl}, kJ/mol	ΔS_m^{cl}, J/(mol·K)	ΔG_m^{cl}, kJ/mol
			Trimer 2				
$C_5H_{13}COOH$	−76.70	−351.23	27.96	$C_{11}H_{25}COOH$	−138.36	−495.67	9.34
$C_6H_{15}COOH$	−92.14	−382.65	21.90	$C_{12}H_{27}COOH$	−154.21	−524.58	2.12
$C_7H_{17}COOH$	−96.93	−388.64	18.88	$C_{13}H_{29}COOH$	−159.06	−538.45	1.40
$C_8H_{19}COOH$	−112.80	−427.09	14.48	$C_{14}H_{31}COOH$	−174.92	−577.82	−2.73
$C_9H_{21}COOH$	−117.71	−451.88	16.95	$C_{15}H_{33}COOH$	−179.70	−591.19	−3.52
$C_{10}H_{23}COOH$	−133.47	−486.77	11.58				
			Trimer 3				
$C_5H_{13}COOH$	−59.84	−469.60	80.11	$C_{11}H_{25}COOH$	−145.24	−604.94	35.03
$C_6H_{15}COOH$	−62.22	−466.90	76.92	$C_{12}H_{27}COOH$	−147.39	−594.70	29.84
$C_7H_{17}COOH$	−88.17	−514.21	65.07	$C_{13}H_{29}COOH$	−173.70	−650.43	20.13
$C_8H_{19}COOH$	−90.45	−510.95	61.82	$C_{14}H_{31}COOH$	−175.87	−646.86	16.89
$C_9H_{21}COOH$	−116.75	−560.19	50.19	$C_{15}H_{33}COOH$	−202.20	−684.89	1.90
$C_{10}H_{23}COOH$	−118.92	−553.96	46.16				
			Trimer 4				
$C_5H_{13}COOH$	−60.25	−439.43	70.71	$C_{11}H_{25}COOH$	−131.63	−629.87	56.07
$C_6H_{15}COOH$	−63.43	−465.21	75.20	$C_{12}H_{27}COOH$	−135.01	−619.48	49.60
$C_7H_{17}COOH$	−83.93	−509.30	67.84	$C_{13}H_{29}COOH$	−155.52	−683.66	48.21
$C_8H_{19}COOH$	−87.29	−522.77	68.50	$C_{14}H_{31}COOH$	−158.86	−678.36	43.29
$C_9H_{21}COOH$	−107.77	−572.52	62.84	$C_{15}H_{33}COOH$	−179.38	−736.99	40.24
$C_{10}H_{23}COOH$	−111.14	−576.03	60.52				
			Tetramer 1				
$C_5H_{13}COOH$	−160.96	−626.10	25.62	$C_8H_{19}COOH$	−240.13	−752.07	−16.01
$C_6H_{15}COOH$	−199.31	−694.17	7.55	$C_9H_{21}COOH$	−242.70	−720.75	−27.92
$C_7H_{17}COOH$	−201.78	−684.47	2.19	$C_{10}H_{23}COOH$	−281.13	−804.37	−41.43
			Tetramer 2				
$C_5H_{13}COOH$	−124.12	−652.87	70.43	$C_9H_{21}COOH$	−205.82	−792.75	30.42
$C_6H_{15}COOH$	−144.14	−684.40	59.81	$C_{10}H_{23}COOH$	−226.26	−823.79	19.22
$C_7H_{17}COOH$	−164.82	−723.31	50.72	$C_{11}H_{25}COOH$	−246.91	−856.36	8.29
$C_8H_{19}COOH$	−185.15	−752.46	39.08				
			Tetramer 3				
$C_5H_{13}COOH$	−118.27	−531.77	40.20	$C_9H_{21}COOH$	−180.34	−681.29	22.68
$C_6H_{15}COOH$	−142.17	−586.56	32.62	$C_{10}H_{23}COOH$	−204.33	−731.35	13.62
$C_7H_{17}COOH$	−149.26	−604.95	31.02	$C_{11}H_{25}COOH$	−211.45	−755.58	13.71
$C_8H_{19}COOH$	−173.23	−656.92	22.53				

both between the carboxyl groups as a single unit, and between their CO and OH constituents.

The dipole−dipole interaction energy is calculated as (see, e.g., refs 18 and 23):

$$E^{d} = \frac{\mu_R \mu_T}{4\pi\epsilon\epsilon_0 r^3}[2\cos\theta_R \cos\theta_T + \sin\theta_T \cos\varphi] \qquad (2)$$

where μ_R and μ_T are the dipole moments of the subsystems R and T, respectively, r is the distance between the dipoles, θ_R and θ_T are the angles between the axes of R or T subsystems, respectively, and the straight line which connects the subsystems, and φ is the dihedral angle formed by the planes which enclose the R and T subsystems; see Figure 5. The values of charges, angles and distances for the studied clusters could be easily determined using the interactive functions implemented in the WinMopac and HyperChem-7 software.

It was found by the analysis of dipole−dipole interaction energy E^d between the carboxyl groups as whole entities that, depending on the mutual position of the groups, the contributions to the cluster formation enthalpy can vary in the magnitude, and even in the sign. For example, for the dimers 1−4 and 6 these values are negative, and for the dimers 5 and 7−9 the values are positive. This fact can be regarded as theoretical background for the use of dipole−dipole interaction energies for the identification and selection of interactions which should be accounted for in the development of the additive scheme, and for the ranking of the contributions into the relevant (which should be accounted for) and irrelevant (which could be neglected) ones in the framework of the proposed approach.

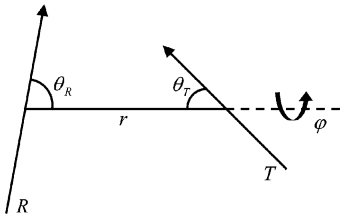

Figure 5. Schematic representation of the relative position of interacting systems via dipole moment vectors.

Comparing the E^d values for dimer 1 and dimer 4 one can see that, although dimer 1 involves two intermolecular hydrogen bonds, whereas in dimer 4 only one such bond is present. The E^d value for dimer 1 is lower than that for dimer 4, because the length of dipoles in dimer 1 is essentially smaller than in dimer 4. It follows therefore that the interaction between carboxyl groups in dimer 1 differs in its character from that in dimer 4, and these interactions should be accounted for separately. Also, the dipoles of carboxyl groups which involve the intramolecular interaction are essentially different, both in magnitude and in direction, from the dipoles of carboxyl groups which do not participate in these interactions. Therefore, the interactions which involve the intramolecular hydrogen bonds should also be accounted for separately.

A detailed distinction between the interactions of carbonyl groups, i.e., the decomposition of their dipoles into the sum of dipoles related to the carbonyl and hydroxyl constituents, enables us to reveal other types of interactions between the carbonyl and hydroxyl groups and to determine the criterial threshold for these interactions. According to eq 2, this threshold is

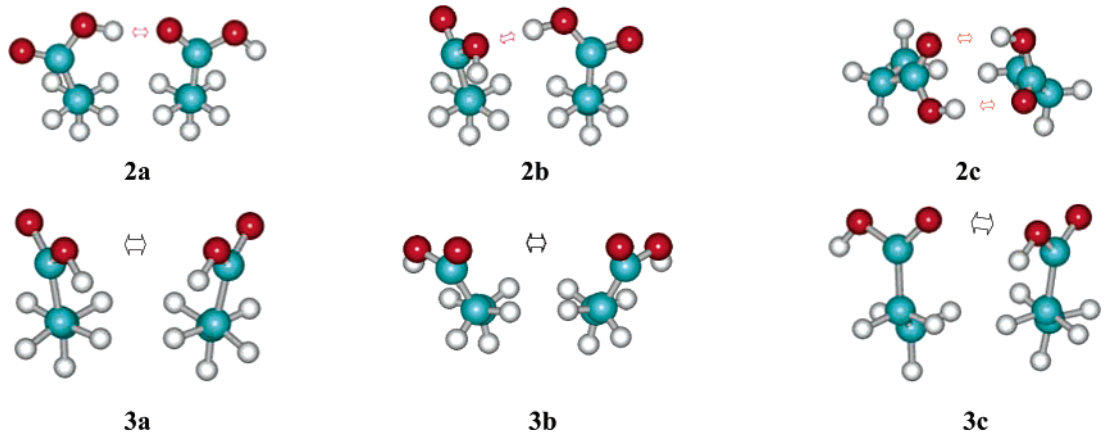

Figure 6. Various types of interactions between hydrogen and oxygen atoms: 2a, intermolecular hydrogen bond (CO−HO); 2b, (HO−HO) interaction; 2c, double intermolecular hydrogen bond (double); 3a, (HO−OH) interaction; 3b, (CO−OC) interaction; 3c, (CO−OH) interaction.

TABLE 4: Number and Types of Intermolecular Interactions in Clusters

cluster	k_a	k_b	n_{CO-HO}	n_{HO-HO}	n_{CO-OC}	$n_{\{HO-OH/CO-OH\}}$	n_{double}	$n_{bicyclic}$
dimer 1	$\{n/2\}$						1	
dimer 2	$\{(n+1)/2\}$		1					
dimer 4	$\{n/2\}$		1					
dimer 6		n	1					
dimer 7		n			1			
dimer 9		n		1				
trimer 1	$3\{n/2\}$		3			3		
trimer 2	$2\{n/2\}$		2					
tetramer 1	$4\{n/2\}$		4			4		
tetramer 2	$2n$						2	1
tetramer 3	$3\{n/2\}$		3					
lacuna 1	$\{(n-1)/2\}+\{n/2\}$				2	2		
lacuna 2	$2\{(n+1)/2\}$							1

proportional to μ^2/r^3 (the numerical value of the threshold could be assumed to be 0.001 μ^2/r^3 with the dipole moment expressed in Debye and the distance in Å). As the maximum value of the term enclosed in square brackets in eq 2 is 2, then from the critical threshold value for various types of interactions it becomes possible to estimate the limiting distances between the interacting subsystems, above which the corresponding interactions could be disregarded. In particular, for the CO−OC, CO−OH, and HO−OH interactions these distances are 7.4, 6.7, and 6.1 Å, respectively. The types and numbers of significant interactions in the studied clusters are listed in Table 4. This table (and also the correlations calculated on its basis) does not include the clusters possessing intramolecular hydrogen bonds, because these clusters are formed spontaneously at larger alkyl chain length than the clusters with intermolecular hydrogen bonds. Similarly, the correlations do not involve trimer 3 and trimer 4, for which the spontaneous formation of clusters takes also place at large n values; see Table 3.

When selecting the significant interactions in the clusters, one should take into account not only the separation between the interacting groups, but also their mutual positions. For example, in the tetramer 1 the distance between the nearest carbonyl groups which belong to neighboring monomers (3.8 Å) is significantly lower than the distance between other interacting groups, e.g., OH and OH (4.17 Å) or CO and OH (4.66 Å). Also, the dipole moment of the CO group is essentially higher than that of the hydroxyl group. Nevertheless, it follows from the analysis of the dipole−dipole interactions that, in the present case, the CO−OC interactions are insignificant because of their relative positions.

It is seen from Table 4 that, in addition to the three types of interaction between hydrogen atoms of alkyl groups (cf. ref 10), also some oxygen−hydrogen and oxygen−oxygen interactions should be taken into account. It is seen from Figure 6 that the 2a type interaction arises between the carbonyl oxygen and hydroxyl hydrogen which belong to different molecules, if oriented properly, whereas the 2b type interaction takes place between the hydroxyl oxygen and hydroxyl hydrogen which belong to different molecules. In dimer 1, a specific type of intermolecular interaction between two carboxyl groups exists, which leads to the formation of two intermolecular hydrogen bonds, and it was mentioned above that the specific factor n_{double}: 2c interaction type should be introduced to account for this interaction.

In addition to these interactions, for the analysis of entropies it is necessary to account for the interactions between the oxygen atoms which belong to different molecules in the cluster of the types 3a, 3b, and 3c; cf. Figure 6. The 3a type interaction, similarly to the 2c type, was introduced in ref 10 where the cluster formation in alcohols was considered. The interaction between oxygen carbonyl atoms corresponds to the 3b type of oxygen−oxygen interactions. The 3c type corresponds to the interaction between the carbonyl and hydroxyl groups, see Figure 6. It should be noted that some of these interactions are present in the same combinations in different clusters, and therefore to increase the reliability in the description of thermodynamic functions these interactions could be incorporated into single parameters. For example, $n_{bicyclic}$, which characterizes the interaction between the functional groups of dimers in tetramer 2, is involved in the same form into the interlayer lacunas of large and infinite clusters formed on the basis of the trimer 1 and tetramer 1 structures. A similar situation exists for HO−OH and CO−OH interactions which enter in the same combinations the trimer 1 and tetramer 1, and the

interlayer lacunas of large and infinite clusters based on the dimer 4 structures, see $n_{\{\mathbf{HO-OH/CO-OH}\}}$ in Table 4. The interlayer lacuna 2 corresponds to infinite clusters based on trimer 1 and tetramer 1.

The analysis summarized above enables one to determine the number of the interactions of each type indicated for each of the clusters considered (see Table 4), to subtract the contributions of methylene fragments on the basis of the additive scheme,[10] and to build the corresponding multiparametric regression. This leads to the formulas for the calculation of enthalpy and entropy of clusterization:

$$H_m^{\,\mathrm{cl}} = -(9.20 \pm 0.08)k_a - (5.85 \pm 0.15)k_b - (20.74 \pm 0.26)n_{\mathrm{CO-HO}} - (28.22 \pm 1.42)n_{\mathrm{double}} - (18.33 \pm 3.35)n_{\mathrm{bicyclic}} \quad (3)$$

$$(R = 0.98;\ S = 4.71\ \mathrm{kJ/mol};\ n = 108)$$

$$\Delta S_m^{\,\mathrm{cl}} = -(18.4 \pm 0.6)k_a - (20.4 \pm 0.7)k_b - (147.7 \pm 1.5)n_{\mathrm{CO-HO}} - (136.3 \pm 5.2)n_{\mathrm{HO-HO}} - (163.8 \pm 5.2)n_{\mathrm{double}} - (101.4 \pm 5.2)n_{\mathrm{CO-OC}} + (41.7 \pm 1.9)n_{\{\mathrm{HO-OH/CO-OH}\}} - (133.1 \pm 12.2)n_{\mathrm{bicyclic}} \quad (4)$$

$$(R = 0.991;\ S = 17.2\ \mathrm{J/(mol\cdot K)};\ n = 108)$$

where k_a and k_b are the numbers of a certain type of contacts between the interacting alkyl groups in a cluster, $n_{\mathrm{CO-HO}}$, $n_{\mathrm{HO-HO}}$, n_{double} are the numbers of oxygen−hydrogen interactions (see 2a−2c interactions, Figure 6), $n_{\{\mathrm{HO-OH/CO-OH}\}}$, $n_{\mathrm{CO-OC}}$ are the numbers of unshared pairs of oxygen atoms, cf. 3a−3c interactions, Figure 6. The values of parameters k_a and k_b were taken from ref 10. Therefore, the correlation coefficients and standard deviations indicated above describe only the interactions between the atoms of carboxyl groups. It is seen that the values of correlations are quite satisfactory. High standard deviation for $\Delta S_m^{\,\mathrm{cl}}$ is caused, similarly to the case of alcohols, by a more complicated entropy dependence on the cluster structure, which cannot be reduced to the O−H, O−O contributions only.

Using the correlations eqs 3 and 4 it is possible to estimate enthalpies and entropies of the cluster formation (also for infinite clusters) only on the basis of the molecular geometry of a cluster (the relative location of methylene and carboxyl groups), the number of methylene fragments in the monomer (n) and the number of molecules involved in the cluster (m). Consider first rectangular clusters formed by dimers 4; see Figure 7. Figure 8a illustrates the dependence of enthalpy per one monomer molecule $\Delta H_m^{\,\mathrm{cl}}$ for linear clusters formed by this dimer which is characterized by the 1a type of H−H interactions between the alkyl chains. Such clusters can be regarded as the initial terms in the series of large and infinite plane clusters. Similar to that found for alcohols, a successive decrease of clusterization enthalpies of these clusterstakes place with the increase of the number of molecules in a cluster; this is due to the increase of the number of intermolecular interactions per one molecule in the cluster. Finally, for sufficiently large clusters the $\Delta H_m^{\,\mathrm{cl}}/m$ ratio attains a certain constant value. A similar dependence exists also for the relative cluster formation entropy $\Delta S_m^{\,\mathrm{cl}}/m$, see Figure 8b. The points shown in Figure 8 indicate the results of quantum chemical calculations, whereas the lines correspond to the calculations according to eqs 3 and 4.

Similar dependencies exist also for other families of clusters, e.g., for those formed by trimer 1. The proposed approach

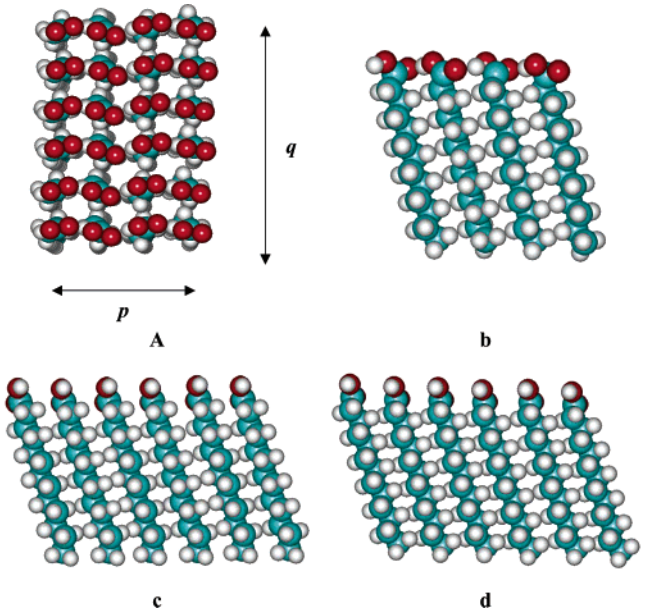

Figure 7. Structure of the finite $p\cdot q$ cluster formed by dimer 4: (a) view from above; (b) view in the q direction; (c) cross-section along the first (every odd) layer in the p direction; (d) cross-section along the second (every even) layer in the p direction.

enables one to derive analytical expressions for the clusterization enthalpy and entropy for plane regular clusters of any size and shape. For example, for the rectangular cluster $p\cdot q$ (see Figure 7) one obtains

$$k_a = \left\{\frac{n}{2}\right\}q(p-1) + (q+1)\left[\left\{\frac{p+1}{2}\right\}\left\{\frac{n-1}{2}\right\} + \left\{\frac{p}{2}\right\}\left\{\frac{n}{2}\right\}\right] \quad (5)$$

$$n_{\mathrm{CO-HO}} = q(p-1),$$
$$n_{\{\mathrm{HO-OH/CO-OH}\}} = n_{\mathrm{CO-OC}} = p(q-1),$$
$$k_b = n_{\mathrm{HO-HO}} = n_{\mathrm{double}} = n_{\mathrm{bicyclic}} = 0 \quad (6)$$

The expression for k_a is quite complicated. This is because the number of H−H interactions in the even and odd layers of the cluster in the p direction are different, cf. Figure 7. The first term in eq 5 represents the number of H−H interactions in each layer in the p direction multiplied by the number of these layers (q). The second term expresses the number of interactions which exist in the q direction. Here the first and second terms in square brackets correspond to the number of interactions in the even and odd layers, respectively. Introducing k_a and $n_{\mathrm{CO-HO}}$ values into the expressions eqs 3 and 4 one can calculate entropy and enthalpy for any cluster with arbitrary q, p, and n values.

The limiting value for the expression eq 5 which correspond to an infinite cluster could be obtained using the relations for the integer part of a number: $\{n + {}^1/_2\}\{n/2\} = n$; $\{n/2\} + {}^1/_2(1 + (-1)^{n+1}/2$. Introducing these relations into eq 5, one obtains

$$k_a = pq(n-1) - q\left\{\frac{n}{2}\right\} - p\left\{\frac{n-1}{2}\right\} + \frac{(q-1)p}{2}\left(\frac{1+(-1)^n}{2}\right) - \frac{q-1}{2}\left(\frac{1+(-1)^{p+1}}{2}\right)\left(\frac{1+(-1)^n}{2}\right) \quad (7)$$

From eq 7, enthalpy, entropy, and Gibbs' energy of clusterization for various infinite clusters can be calculated. For example,

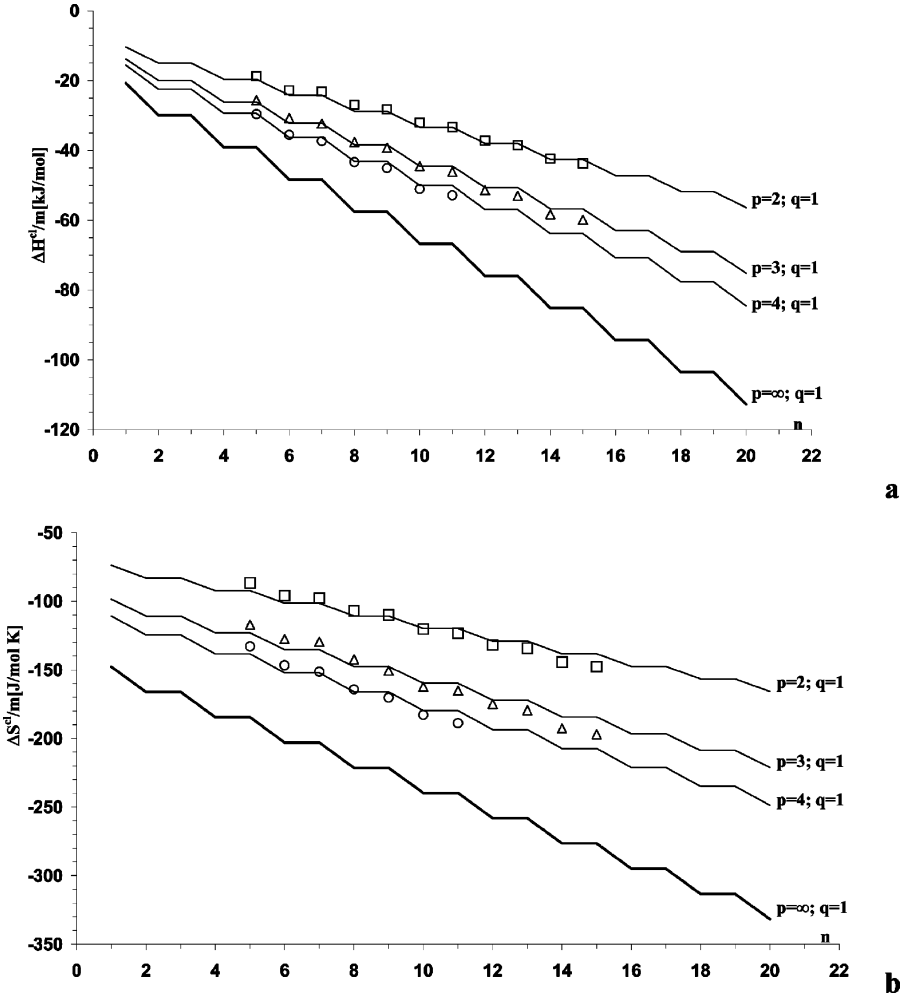

Figure 8. Clusterization enthalpy and entropy per one monomer for linear clusters formed by dimer 4.

for an infinite cluster in the p direction (i.e., $q = 1$, $p \rightarrow \infty$) one obtains the values per one monomer:

$$k_{a\infty} = \left\{\frac{n}{2}\right\}, \quad n_{CO-HO\infty} = 1,$$
$$n_{\{HO-OH/CO-OH\}\infty} = n_{CO-OC\infty} = 0$$
$$k_{b\infty} = n_{HO-OH\infty} = n_{double} = n_{bicyclic\infty} = 0 \qquad (8)$$

Then from eqs 3, 4, and 8, the thermodynamic parameters for this infinite linear cluster (per one monomer) are expressed as follows: $\Delta H_\infty^{cl} = -9.20\{n/2\} - 20.74$ kJ/mol, $\Delta S_\infty^{cl} = -18.4\{n/2\} - 147.7$ J/(mol·K), and Gibbs' energy of the cluster formation $\Delta G_\infty^{cl} = \Delta H_\infty^{cl} - T\Delta S_\infty^{cl} = -3.7\{n/2\} + 23.3$ kJ/mol.

For linear clusters infinite in the q direction ($q \rightarrow \infty$, $p = 1$), one obtains from eqs 5 and 6 the following values per one monomer:

$$k_{a\infty} = \left\{\frac{n-1}{2}\right\}, \quad n_{CO-HO\infty} = 0,$$
$$n_{\{HO-OH/CO-OH\}\infty} = n_{CO-OC\infty} = -\frac{1}{q}$$
$$k_{b\infty} = n_{HO-HO\infty} = n_{double\infty} = n_{bicyclic\infty} = 0 \qquad (9)$$

and from eqs 3 and 4 the expressions for the thermodynamic properties are

$$\Delta H_\infty^{cl} = -9.20\left\{\frac{n-1}{2}\right\}\text{kJ/mol},$$
$$\Delta S_\infty^{cl} = -18.4\left\{\frac{n-1}{2}\right\}\text{J/(mol·K)}$$

and

$$\Delta G_\infty^{cl} = 3.7\left\{\frac{n-1}{2}\right\} + 17.8 \text{ kJ/mol}$$

It is seen from Figure 9 that the ΔG_∞^{cl} dependencies for ($q = 1$, $p \rightarrow \infty$) and ($q \rightarrow \infty$, $p = 1$) are steplike, and shifted with respect to each other by unity along the n axis. This fact could be easily explained by noting that the Gibbs' energy for the cluster which involves the hydrogen bond is proportional to $\{n/2\}$, whereas for the cluster without the hydrogen bond this energy is proportional to $\{n - 1/2\}$.

For plane two-dimensional infinite clusters ($p \rightarrow \infty$, $q \rightarrow \infty$) see Figure 7, one obtains

$$k_{a\infty} = (n+1) + \frac{1}{4}[1 + (-1)^n], \quad n_{HO-OH/CO-OH\infty} = n_{CO-OC\infty}$$
$$k_{b\infty} = n_{HO-HO\infty} = n_{double\infty}\, n_{bicyclic\infty} = 0 \qquad (10)$$

Introducing these values into eqs 3 and 4 one obtains for the Gibbs' energy per one monomer the expression: $\Delta G_\infty^{cl} = -3.7(n-1) - 0.9[1 + (-1)^n] + 41.1$ kJ/mol. By analysis of this relation, it can be shown that these clusters are formed spontaneously for $n \geq 13$.

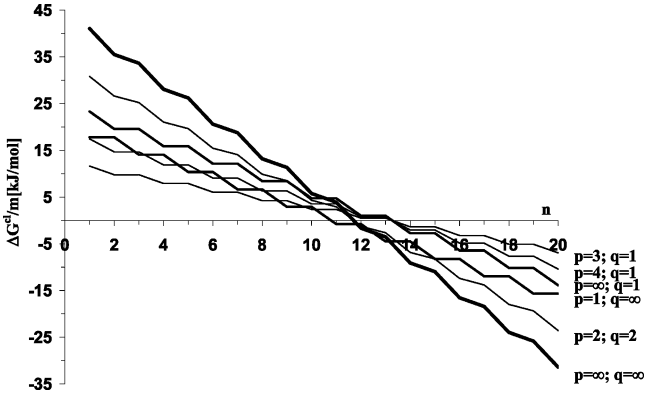

Figure 9. Clusterization Gibbs' energy per one monomer for plane clusters formed by dimer 4.

It follows from Figure 9, which shows the dependence of ΔG_{∞}^{cl} per one monomer on the alkyl chain length, that all the curves intersect the abscissa axis in the interval $11 > n > 14$. Therefore, spontaneous aggregation leading to the formation of plane rectangular clusters can take place at $n \geq 13$.

From the analysis of Table 3 one can see that the values of free clusterization energy per one monomer for the cyclic trimer 1 and tetramer 1 structures are lower than the corresponding values for $p\cdot q$ infinite cluster. Therefore, it seems probable that the infinite cluster should be decomposed into cyclic trimers and tetramers. At the same time, the infinite cluster does not contain any structural units which correspond to cyclic trimers and tetramers, and the decomposition of bonds in this cluster can result only in the formation of the linear clusters dimer 4, dimer 2, and tetramer 3, which are less preferable (with respect to energy per one monomer) than the infinite cluster. Thus, the $p\cdot q$ infinite cluster, once formed, will not be decomposed into cyclic trimers and tetramers. Therefore, for $8 \geq n \geq 12$ the formation of cyclic trimers and tetramers is possible, while for $n > 12$ the formation of $p\cdot q$ infinite clusters formed by monomer 2 will take place. In this case, the formation of cyclic dimers from monomer 2 is less preferable energetically, whereas the formation of dimers and trimers seems to be less probable because of the kinetic control of the process.

The formation of cyclic tetramers (tetramer 1) may be thought of as a two-stage process: opening of the cyclic trimers (trimer 1), i.e., disconnection of one hydrogen bond and $\{n/2\}$H−H bonds, followed by the attachment of corresponding monomers (monomer 2) to these opened entities. Under kinetic consideration, this process is governed by the activation free energy $\Delta G^{\#}$, which is close to the Gibbs' energy corresponding to the opening of the cyclic trimer. This energy could be estimated from the additive scheme (eqs and 4) as $\Delta G^{\neq} = 3.7\{n/2\} - 10.84$ kJ/mol. Therefore, for $n \geq 6$ the activation energy becomes positive, and the formation of cyclic trimers is nonfavorable from the kinetic point of view.

A significant role in the cluster formation plays the interface, which determines a certain spatial orientation of the monomer. At the current stage, this factor is disregarded in quantum chemical calculations. Note that the cyclic clusters trimer 1 and tetramer 1 are oriented perpendicularly to the interface, whereas linear clusters dimer 4, trimer 2, tetramer 3, and $p\cdot q$ infinite cluster are inclined with a ~80° angle to the interface.

Besides the infinite clusters formed by clusterization of monomers as described above, the formation of large and infinite clusters by clusterization of larger molecular aggregates (e.g., cyclic trimers and tetramers) is probable. Note that, from kinetic considerations, this way of the formation of such clusters is less probable than their formation from monomers. Next we consider some examples describing the thermodynamic parameters of the cluster formation in these structures.

Not only hexamers but also the hexagonal clusters which could be then infinitely extended, can be built on the basis of trimer 1. The fragments of such an infinite hexagonal cluster are shown in Figure 10, ranged according to the increase of their dimensions. The distribution of different types of interactions and the total number of monomers (m) in these clusters depend on the number of layers (r) in the fragment as

$$k_a = 6r\{n/2\} + 6r(3r-1)n,$$
$$n_{CO-HO} = n_{(HO-OH/CO-OH)} = 18r^2, \quad n_{bicylic} = 3(3r^2 - r)$$
$$k_b = n_{HO-HO} = n_{double} = N_{CO-OC} = 0, \quad m = 18r^2 \quad (11)$$

Proceeding to the limit $r \rightarrow \infty$, one obtains the expressions for various types of interactions per one monomer in an infinite hexagonal cluster:

$$k_{a\infty} = n, \quad n_{CO-HO\infty} = n_{\{HO-OH/CO-OH\}\infty} = 1$$
$$n_{bicyclic\infty} = 0.5k_{b\infty} = n_{HO-HO\infty} = n_{double\infty} = n_{CO-OC\infty} \quad (12)$$

From the additive schemes (eqs and 4 and eq 12) one can obtain $\Delta H_{\infty}^{cl} = -9.20n - 11.58$ kJ/mol, $\Delta S_{\infty}^{cl} = -18.4n - 172.6$ J/(mol·K) and $\Delta G_{\infty}^{cl} = -3.7n + 39.8$ kJ/mol. From the analysis of the expression for ΔG_{∞}^{cl} and the graphical dependence shown in Figure 11, one can conclude that, for pentadecane acid ($n = 15$) and its homologues with longer alkyl chain, spontaneous formation of plane infinite clusters possessing hexagonal structure can take place. It was noted above that for finite hexagonal clusters the dependencies of the clusterization thermodynamic parameters on n is steplike, whereas for infinite clusters this dependence is linear. This is because eq 11 which expresses the k_a value for finite clusters combines two terms: one term, dependent on $\{n/2\}$, corresponds to a steplike dependence, and the other term is linearly dependent on n. As the second term is proportional to r^2, whereas the first term is proportional to r, the stepwise dependence prevails for small m values, that becomes negligible with the increase of m.

With tetramer 1 chosen as structural-forming unit, a two-dimensional rectangular $t\cdot s$ large and infinite clusters can be built, see Figure 12. The expressions for the dependence of distribution of various types of interactions and total number of monomers (m) in these clusters on the cluster size, i.e., on t, s, and n values are

$$k_a = 4ts\left\{\frac{n}{2}\right\} + 2(t-1)s\left\{\frac{n+1}{2}\right\} 2t(s-1)\left\{\frac{n+1}{2}\right\},$$
$$n_{CO-HO} = n_{\{HO-OH/CO-OH\}} = 4ts$$
$$n_{bicyclic} = [(t-s)s + t(s-1)],$$
$$k_b = n_{HO-HO} = n_{double} = n_{CO-OC} = 0, \quad m = 45ts \quad (13)$$

For this case the ($t = 1$, $s \rightarrow \infty$) and ($t \rightarrow \infty$, $s = 1$) clusters are equivalent to each other, and the distribution of intermolecular interactions in the clusters is given by the following expressions:

$$k_{a\infty} = n - \frac{1}{2}\left\{\frac{n+1}{2}\right\}, \quad n_{CO-HO\infty} = n_{\{HO-OH/CO-OH\}\infty} = 1$$
$$n_{bicyclic} = 0.25, \quad k_{b\infty} = n_{HO-OH\infty} = n_{double\infty} = n_{CO-OC\infty} = 0 \quad (14)$$

Using the additive schemes (eqs and 4 and the relations eq 14),

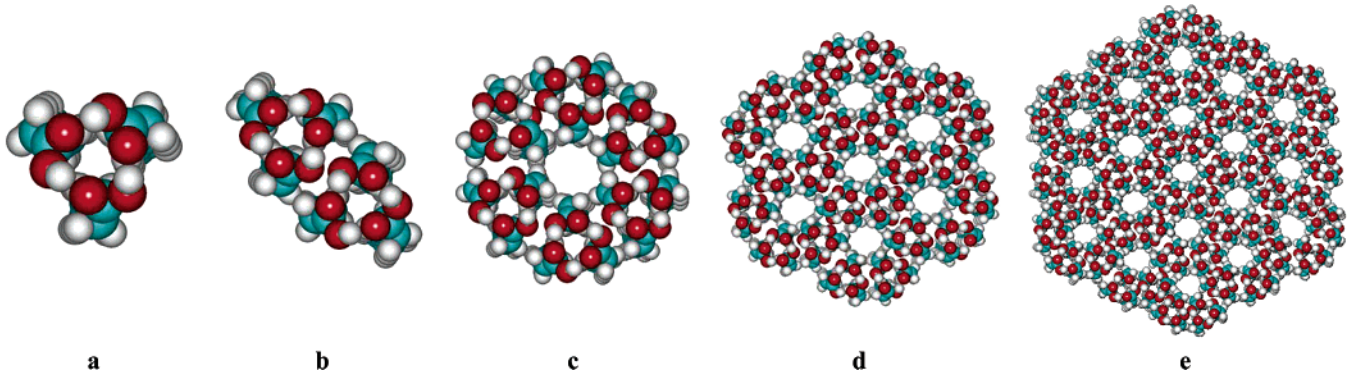

Figure 10. Small and large clusters formed by trimer 1 (view from above): (a) trimer 1; (b) hexamer; (c) first layer of the hexagonal infinite cluster ($r = 1$); (d) first two layers of the hexagonal infinite cluster ($r = 2$); (e) first three layers of the hexagonal infinite cluster ($r = 3$).

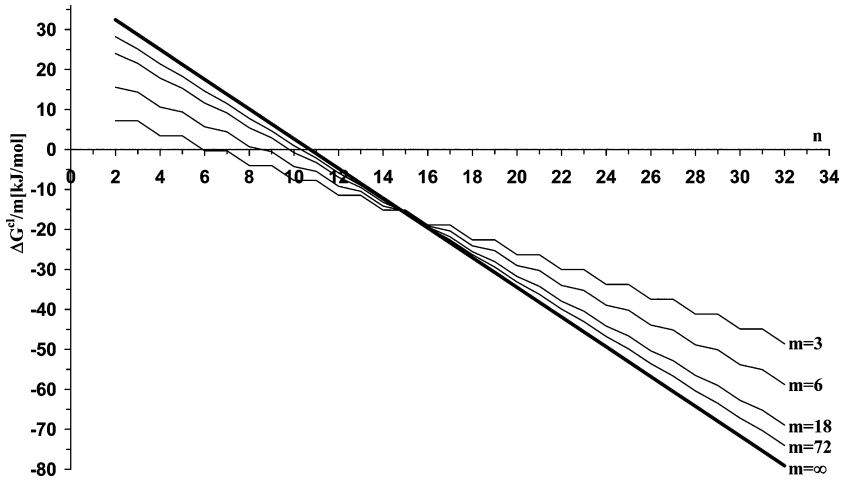

Figure 11. Clusterization Gibbs' energy per one monomer for hexagonal clusters formed by trimer 1.

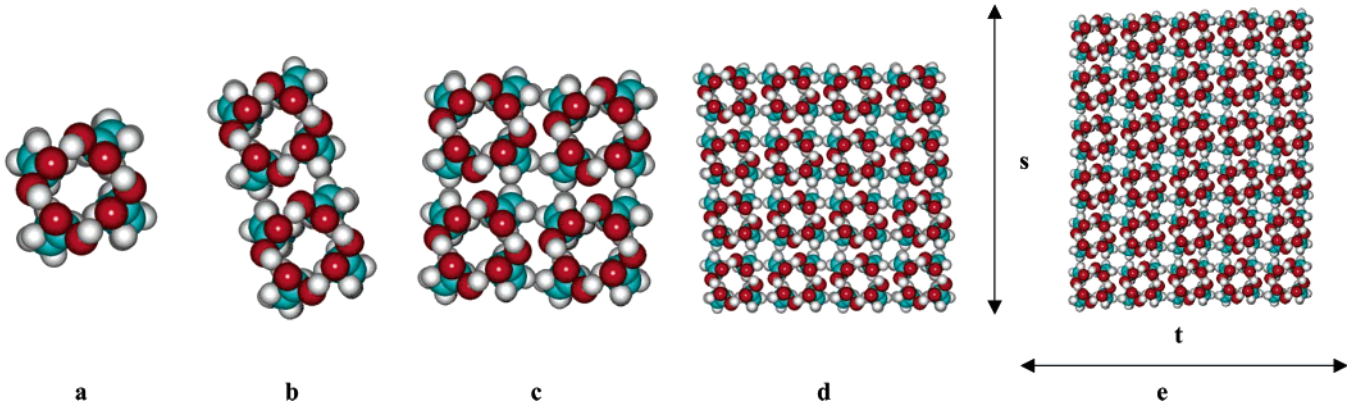

Figure 12. Clusters formed by tetramer 1: (a) tetramer 1 ($t = 1$; $s = 1$); (b) octamer ($t = 2$; $s = 1$); (c) hexadecamer ($t = 2$; $s = 2$); (d) tetrahexacontamer ($t = 4$; $s = 4$); (e) rectangular cluster (t; s).

for the infinite monomolecular band-like clusters formed by the tetramer 1 structure, one obtains the values of thermodynamic functions per one monomer: $\Delta H_{\infty}^{cl} = -9.20n$ kJ/mol, $\Delta S_{\infty}^{cl} = -18.4n - 139.3$ J/(mol·K), and $\Delta G_{\infty}^{cl} = -3.7n + 25.3$ kJ/mol.

For the infinite rectangular plane t·s cluster, in the limit $t \rightarrow \infty$, $s \rightarrow \infty$ one obtains from eq 4 the values per one monomer:

$$k_{a\infty}\ \mathrm{n}, \quad n_{CO-HO\infty} = n_{\{HO-OH/CO-OH\}\infty} = 1$$
$$n_{bicyclic\infty} = 0.5, \quad k_{b\infty} = n_{HO-HO\infty} - n_{CO-OC\infty} = 0 \quad (15)$$

Using the additive schemes (eqs and 4 and the relations eq 15), for such clusters one obtains $\Delta G_{\infty}^{cl} = -3.7n + 39.8$ kJ/mol. It can be seen that eqs 13 and 15 are identical to each other; therefore, the thermodynamic characteristics of the infinite hexagonal and rectangular t·s clusters are the same. It is seen from Figure 13 that, although the ΔG_{∞}^{cl} values become negative at $n \geq 11$, until $n = 15$ the spontaneous decomposition of infinite clusters to tetramers is more preferable, and only for $n \geq 15$ the spontaneous formation of plane two-dimensional rectangular t·s cluster occurs. A similar effect takes place also for infinite hexagonal cluster.

Comparison with Experiments and Thermodynamic Models. The model for aggregation in the adsorption layer[5] with the arbitrary aggregation number m is described by the following

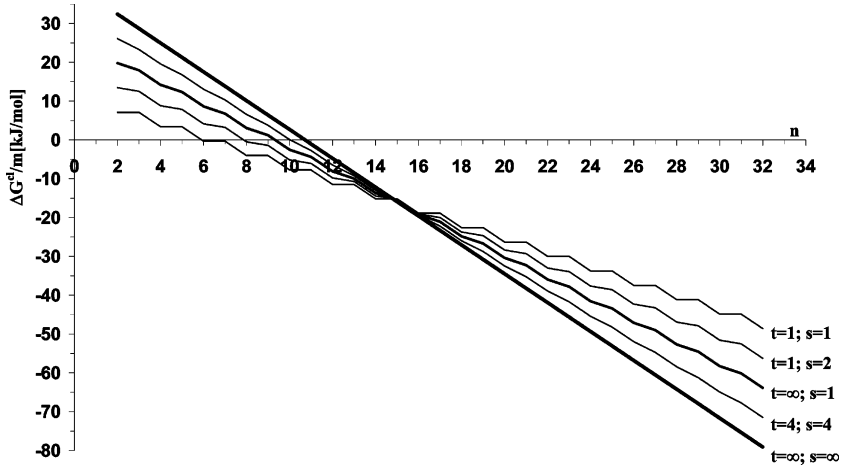

Figure 13. Clusterization Gibbs' energy per one monomer for rectangular *t*·*s* clusters formed by tetramer 1.

equation of state and adsorption isotherm[24−26]

$$-\frac{\Pi\omega}{RT} = in\{1 - 1\omega[1 + (\Gamma_1/\Gamma_c)^{m-1}]\} \qquad (16)$$

$$bc = \frac{\Gamma_1\omega}{\{1 - \Gamma_1\omega[1 + (\Gamma_1/\Gamma_c)^{m-1}]^{\omega_1/\omega}\}} \qquad (17)$$

where R is the gas law constant, T is the temperature, $\Pi = \gamma_0 - \gamma$ is the surface pressure, γ_0 and γ are the surface tensions of solvent and solution, respectively, ω is the partial molar surface areas of the monomer, b is the adsorption constant, c is the surfactants concentration in the solution bulk, Γ_1 and Γ_c are the current and critical adsorption of monomers, respectively, and the average molar area ω is given by

$$\frac{\omega}{\omega_1} = \frac{1 + m(\Gamma_1/\Gamma_c)^{m-1}}{1 + (\Gamma_1/\Gamma_c)^{m-1}} \qquad (18)$$

The equations above are approximate because they disregard the entropy nonideality of surface layer caused by the presence of molecules with different size.[27,28] The equations of state and adsorption isotherm for such systems derived in ref 28 can be modified for the case, that the aggregation of molecules within the surface layer takes place, i.e., in the presence of aggregates and monomers in the surface layer. In particular, using the model of ref 28, we can obtain the following

equation of state:

$$\Pi = \frac{RT}{\omega_1}\left[\ln[1 - \omega_1\Gamma_1 - m\omega_1\Gamma_m] + \omega_1 m\Gamma_n\left(1 - \frac{1}{m}\right)\right\} \qquad (19)$$

The second term in the right-hand side of eq 19 corresponds to

adsorption isotherm equation for monomers:

$$bc = \frac{\Gamma_1}{[1 - \Gamma_1\omega_1 - m\omega_1\Gamma_m]} \qquad (20)$$

equation for the adsorption of aggregates:[24]

$$\Gamma_m = \Gamma_1\left(\frac{\Gamma_1}{\Gamma_c}\right)^{m-1} \qquad (21)$$

the contribution of nonideal entropy to the surface pressure.

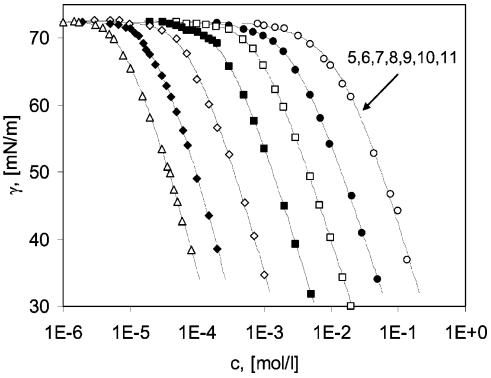

Figure 14. Dependence of surface tension for aqueous solutions of normal fatty acids (C5−C11) on concentration according to data.[8] Theoretical curves calculated from eqs 19−21.

The surface tension isotherms for fatty acids (C_5−C_{11})[8] measured in the presence of 0.005 M HCl (to avoid dissociation) are shown in Figure 14 along with the values calculated from eqs 19−21. The relative root-mean-square error of the calculated surface tension values was within the limit of 0.6−1.5%. For the lower homologues of fatty acids (C_5 and C_6) the Γ_c value is high (approximately equal to the limiting adsorption value). Therefore, the surface layer contains almost no aggregates, whereas for the other homologues the optimum value of the aggregation number n was found to be 3 ± 0.2. The ω_1 values were varied from 1.7×10^5 m^2/mol for C_7 to 1.5×10^5 m^2/mol for C_{11}. When the m value was taken to be 2 or 4, the error related to the calculations according to eqs 19−21 became two times higher. At the same time, when the Frumkin's model was used to describe the results obtained in ref 8, the calculation error was higher by approximately 50−100% for the different homologues. For example, the initial section of the curve for decanoic acid is shown in Figure 15. Here the dotted curve corresponds to Frumkin's equation (the error is equal to 1.4%), and differs essentially both from the experimental curve, and from the calculations made according to the aggregation model (with an error of 0.7%).

In the n range of 7−11, the parameter Γ_c calculated from eqs 19−21 decreases monotonically from 10^{-6} to 10^{-8} mol/m^2. Using the estimate for the Gibbs' energy of trimer formation from monomers: $\Delta G = RT\ln(\omega_1\Gamma_c)$,[9] one obtains the decrease of the Gibbs' clusterization energy in the homologous series of fatty acids from −4 to −12 kJ/mol, with an increment of ca. −2 kJ/mol per one methylene group.

Therefore, the experimental results for the soluble homologues of fatty acids and the thermodynamic models obtained on the

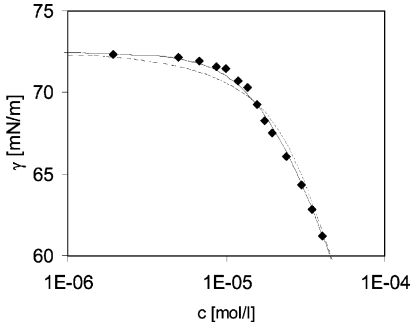

Figure 15. Dependence of surface tension for aqueous solutions of decanoic acid. Dashed curve calculated from Frumkin's model.

basis of the two-dimensional solution theory[27,28] agree well with the predictions which follow from quantum chemical calculations. In the surface layer the trimers are mainly present, and the value of Gibbs' energy for the formation of these aggregates is quite close to that indicated in Figure 11.

Consider next the results obtained for spread monolayers of the higher fatty acid homologues. The experimental $\Pi-A$ (surface pressure vs area per molecule) isotherms for fatty acids $C_{13}-C_{16}$ reported in refs 7 and 29−31 were processed using the theoretical model developed in ref 32 (the so-called generalized Volmer's equation). Using the theory of ref 32 one can calculate the aggregation degree of molecules in the fluid (liquid-expanded) state. Also Gibbs' free energy of condensation can be calculated from the area/molecule in the condensed monolayer and in the critical point of the transition from the fluid (liquid-expanded) to the condensed (liquid-condensed) monolayer.[9,10]

The experimental data reported in refs 7 and 29−31 have shown unambiguously that the formation of large clusters (condensation) occurs at $n = 13$. The same result follows also from the analysis of the Gibbs' energy related to the formation of plane clusters formed by dimer 4 (see Figure 9). The calculations according to the model developed in ref 23 indicate that in the fluid state the C_{13-C16} fatty acids are present in the monolayer in form of dimers or trimers. This result also agrees with conclusions drawn in our study. The experimental estimates of Gibbs' energy regarding to the condensation (transition from trimers to infinite clusters) for the $C_{13}-C_{16}$ fatty acids are −2.2, −3.7, −5.2, and −6.6 kJ/mol, respectively. These values are approximately two times lower than the ΔG_{∞}^{cl} values predicted for the studied clusters by the PM3 method. This fact may possibly be attributed to the approximations involved in the evaluation method[32] and to the overestimation of the hydrogen−hydrogen interactions in the PM3 parametrization. In this regard, it should be noted that the ab initio calculations of the interaction energies in methane and neopentane dimers[33] show that the minima exist at the potential surface of intermolecular interaction energy, which corresponds to hydrogen−hydrogen interactions, but the depths of these minima are smaller than those predicted by the PM3 method.

Conclusions

In the framework of the PM3 molecular orbital approximation, the thermodynamic function characteristics for the formation and geometrical structure of monomers, dimers, trimers, and tetramers of *n*-carboxylic acids are calculated. It is shown that, for the homologues with carbon atom numbers $n \geq 13$, spontaneous aggregation of fatty acids at the air/water interface can take place leading to the formation of infinite plane rectangular clusters whereas for the homologues with $n < 11$ spontaneous decomposition of large aggregates is energetically preferable. At the same time, for the lower homologues ($8 < n < 13$) the formation of trimers is more probable. These results agree well both with the experimental data reported by different authors and with thermodynamic models developed previously for soluble and insoluble monolayers.

The slopes of the regressions calculated for the dependencies of thermodynamic parameters on the hydrocarbon radical chain length for all the clusters considered are quite equal to each other. This fact indicates that the contributions of CH_2 groups to the thermodynamic characteristics of alcohols and acids are the same, and the differences in the formation of clusters by these substances should be attributed only to the differences in the structure and interactions of relevant functional groups. Therefore, both acids and alcohols can be well described in the framework of the developed method, and an extension of the proposed approach to other classes of amphiphilic compounds is suggested.

References and Notes

(1) Malysa, K.; Miller, R.; Lunkenheimer, K. *Colloids Surf.* **1991**, *53*, 47.
(2) Aratono, M.; Uryu, S.; Hayami, Y.; Motomura, K.; Matuura, R. *J. Colloid Interface Sci.* **1984**, *98*, 33.
(3) Lunkenheimer, K.; Hirte, R. *J. Phys. Chem.* **1992**, *96*, 8683.
(4) Lucassen-Reynders, E. H. *J. Colloid Interface Sci.* **1972**, *41*, 156.
(5) Fainerman, V. B.; Miller, R.; Möhwald, H. *J. Phys. Chem. B* **2002**, *106*, 809.
(6) Ter Minassian-Saraga, L. *J. Colloid Sci.* **1956**, *11*, 398.
(7) Boyd, E. *J. Phys. Chem.* **1958**, *62*, 536.
(8) Lunkenheimer, K.; Burzyk, W.; Hirte, R.; Rudert, R. *Langmuir* **2003**, *19*, 6140.
(9) Vysotsky, Yu. B.; Bryantsev, V. S.; Fainerman, V. B.; Vollhardt, D.; Miller, R. *J. Phys. Chem. B* **2002**, *106*, 121.
(10) Vysotsky, Yu. B.; Bryantsev, V. S.; Fainerman, V. B.; Vollhardt, D. *J. Phys. Chem. B* **2002**, *106*, 11285.
(11) Vysotsky, Yu. B.; Bryantsev, V. S.; Fainerman, V B.; Vollhardt, D.; Miller, R. *Colloids Surf. A* **2002**, *209*, 1.
(12) Vysotsky, Yu. B.; Bryantsev, V. S.; Fainerman, V. B.; Vollhardt, D.; Miller, R. *Prog. Colloid Polym. Sci.*. **2002**, *121*, 72.
(13) Vysotsky, Yu. B.; Bryantsev, V. S.; Fainerman, V. B.; Vollhardt, D.; Miller R.; Aksenenko, E. V. *J. Phys. Chem. B* **2004**, *108*, 8330.
(14) Vysotsky, Yu. B.; Bryantsev, V. S.; Fainerman, V. B.; Vollhardt, D.; Miller, R. *Colloids Surf. A* **2004**, *239*, 135.
(15) Vysotsky, Yu. B.; Bryantsev, V. S.; Boldyreva, V. B.; Fainerman, V. B.; Vollhardt, D. *J. Phys. Chem. B*, **2005**, *109*, 454.
(16) Stewart, J. J. P. *MOPAC 2000.00 Manual*; Fujitsu Limited: Tokyo, Japan, 1999.
(17) Mo, O.; Yanez, M.; Elguero, J. *J. Chem. Phys.* **1997**, *107*, 3592.
(18) Hobza, P.; Zahradnic, R. *Intermolecular Complexes. The Role of van der Waals System in Physical Chemistry and in the Biodisciplines*; Academia Praga: Prague, 1988.
(19) Pedley, J. B.; Naylor, R. D.; Kirby, S. P. *Thermochemical Data of Organic Compounds*; Chapman and Hall: London, 1986.
(20) Cox, J. D.; Pilcher, G. *Thermochemistry of Organic and Organometallic Compounds*; Acad. Press: San Diego, CA, 1970; N 4.
(21) Daubert, T. E.; Danner, R. P.; Sibul, H. M.; Stebbins, C. C. *Physical and thermodynamic properties of pure chemicals: Data Compilation, Part 1−Part 5*; Taylor & Francis: Philadelphia, PA, 1998.
(22) Vysotsky, Yu. B.; Bryantsev, V. S.; Miller, R.; Fainerman, V. B.; Vollhardt, D. *The 9th International Conference on Organized Molecular Films (LB 9). Program and Abstracts*; Max Planck Institute of Colloids and Interfaces: Potsdam, Germany, 2000; Vol. 2, p 143.
(23) Israelachvili, J. N. *Intermolecular and surface forces*; Academic Press: San Diego, CA, 1998.
(24) Fainerman, V. B.; Miller, R. *Langmuir* **1996**, *12*, 6011.
(25) Fainerman, V. B.; Lucassen-Reynders, E. H.; Miller, R. *Colloids Surf. A* **1998**, *143*, 141.
(26) Fainerman, V. B.; Miller, R.; Aksenenko, E. V. *J. Phys. Chem. B* **2000**, *104*, 5744.
(27) Defay, R.; Prigogine, I. *Surface Tension and Adsorption*; Longmans, Green: London, 1966.
(28) Fainerman, V. B.; Lucassen-Reynders, E. H.; Miller, R. *Adv. Colloid Interface Sci.* **2003**, *106*, 237.
(29) Smith, T. J. *Colloid Interface Sci.* **1967**, *23*, 27.
(30) Harkins, W. D.; Boyd, E. *J. Am. Chem. Soc.* **1939**, *61*, 1188.
(31) Harkins, W. D.; Fraser, T. Y.; Boyd, E. *J. Chem. Phys.* **1940**, *8*, 954.
(32) Fainerman, V. B.; Vollhardt, D. *J. Phys. Chem. B* **1999**, *103*, 145.
(33) Metzger, T. G.; Ferguson, D. M.; Glauser, W. A. *J. Comput. Chem.* **1997**, *18*, 70.